



On the phenomenon of the blue Sun

Nellie Wullenweber¹, Anna Lange¹, Alexei Rozanov², and Christian von Savigny¹

¹Institute of Physics, University of Greifswald, Felix-Hausdorff-Str. 6, 17489 Greifswald, Germany

²Institute of Environmental Physics, University of Bremen, Otto-Hahn-Allee 1, 28359 Bremen, Germany

Correspondence: C. von Savigny (csavigny@physik.uni-greifswald.de)

Abstract. This study examines the cause of the blue colour of the Sun as observed after the eruption of Krakatoa in 1883 as well as other volcanic eruptions or massive forest fire events. Aerosol particles, e.g., volcanic ash or products of biomass burning are believed to be able to modify the spectral distribution of transmitted solar radiation making it appear blue or green to a human observer.

5 Previous studies already showed that narrow aerosol particle size distributions with radii on the order of about 500 nm can lead to anomalous scattering, i.e., scattering cross sections increasing with increasing wavelength in the visible spectral range. In this work we treat the effect of Rayleigh scattering on the shape of the transmitted solar spectrum correctly employing radiative transfer (RT) simulations with the SCIATRAN RT-model. The colour associated with solar transmission spectra is determined based on the CIE colour matching functions and CIE chromaticity values. It is shown that a blue Sun can be
10 simulated for aerosol optical depths (at 550 nm) of about $\tau = 0.5$ (or higher) if Rayleigh scattering is taken into account. Without considering Rayleigh scattering – as in most of the previous studies – a blue Sun is in principle produced with aerosol optical depths as low as about $\tau = 0.1$ (at 550 nm), if the aerosol particle size distribution is chosen to maximize anomalous scattering in the visible spectral range. It is demonstrated that Rayleigh scattering – as expected – has a strong impact on the transmission spectrum, particularly at low solar elevation angles, and needs to be considered for a correct determination of
15 the perceived colour of the Sun. We also test the hypothesis that the blue Sun after the eruption of Krakatoa was caused by large abundances of water vapour in the atmosphere, as proposed in earlier studies. In addition, we present a case study on a particularly noteworthy blue-Sun-event in the past, i.e., the one related to the large Canadian forest fires in September 1950.

1 Introduction

This work has been inspired by various reports on sightings of the Sun appearing blue. Next to other reports, e.g., after the
20 extensive forest fires in Canada in 1950 (e.g., Gelbke, 1951; Wilson, 1951; Penndorf, 1953) widespread observations of a blue Sun have been made following the eruption of the Krakatoa volcano in 1883 (e.g., Larrabee, 1884; Kiessling, 1888; Symons et al., 1888). Witnesses described the Sun rising in a “splendid green”, and turning “bright blue” near the zenith later during the day in the aftermath of the Krakatoa eruption as noted in Symons et al. (1888). Particularly noteworthy is the book by Kiessling (1888) that provides a comprehensive compilation of unusual atmospheric optical effects associated with the
25 Krakatoa eruption and also during the 2000 years before, including several reports on green and blue suns. Historical reports



on an unusually coloured sun or moon can provide important independent information on exceptional natural events, e.g., volcanic eruptions (e.g., Bauch, 2017).

Unfortunately, particle samples of unusual aerosol layers or reliable experimental evidence such as, e.g., spectral distribution measurements are typically not available for blue Sun events (exceptions are discussed below). For the Sun to appear blue, instead of white or yellowish, the normal spectral distribution of solar radiation has to be modified in a way, that less red light is transmitted to the observer compared to the blue component of light. The suppression of red light in transmitted spectra may in principle be caused by wavelength selective absorption or scattering processes, where absorption could be due to gaseous constituents or aerosols. The latter possibility is unlikely, because absorption coefficients of typical tropospheric aerosols usually decrease with increasing wavelength in the visible spectral range (e.g., Bergstrom et al., 2007). For this reason we focus on the possibility that the effect is caused by aerosol scattering. Previous studies have found that particles in the radius range from 400 – 700 nm (depending on the real part of the refractive index n_r) may lead to anomalous scattering, i.e., scattering coefficients increase with increasing wavelength in the visible spectral range, and could cause the observed effect if the aerosol particle size distribution is sufficiently narrow (Penndorf, 1953; Wilson, 1951; Porch, 1973; Ehlers et al., 2014). These studies, however, typically neglect the effect of Rayleigh scattering by air molecules on the spectral distribution of transmitted solar radiation. Rayleigh scattering suppresses the blue component, making it more difficult to produce a blue Sun.

It is also noteworthy that a blue Sun during a sunset on Mars has been captured in a picture taken by the Mars expedition rover Spirit in 2005, increasing the focus on the aerosol layer of the thin Martian atmosphere in order to find an explanation for the phenomenon (Ehlers et al., 2014).

Aerosol particles vary greatly in size but volcanic sulfate aerosol particles or biomass burning aerosols typically have sizes similar to the wavelength of visible radiation. If the aerosol particles are assumed to be spherical for simplicity, their scattering properties can be calculated according to Gustav Mie's scattering of light theory (Mie, 1908). In this study we assume spherical particles and Mie theory was used to model extinction coefficients of aerosol particles with different particle size distributions.

In this work, the full radiative transfer of solar radiation through the atmosphere was simulated with SCIATRAN, a radiative transfer model developed by the Institute of Environmental Physics of the University of Bremen, Germany (Rozanov et al., 2014). In addition, the colours resulting from the calculated transmission spectra are determined and displayed. The calculated spectral distribution reaching the Earth's surface has to be transformed into a colour on a digital output device, in a way a human with normal eyesight would perceive it. Colour modelling presented by the *International Commission on Illumination (CIE)* and the sRGB colour space was chosen and applied, the resulting colours are presented (CIE, 2004; Stokes et al., 1996).

The paper is structured as follows. Section 2 provides a short summary of the approach and methods used, describing both the radiative transfer model as well as the colour modelling. In section 3 the main results – including an investigation of the effects of Rayleigh scattering and absorption by H₂O as well as a case study based on spectral observations after the intense Canadian wildfires in September 1950 – are presented. Sections 4 and 5 discuss and summarize the findings on possible characteristics of particles responsible for the blue colour of the Sun.



60 2 Methodology

We first describe the Mie simulations and the radiative transfer model employed, followed by a summary of the colour modelling approach used in this study.

2.1 Radiative transfer simulation: Mie scattering calculations and SCIATRAN

In order to model the transmitted solar radiation reaching the Earth's surface, first extinction coefficients of the aerosol particles were calculated using Mie theory and later implemented as an aerosol layer in the radiative transfer model SCIATRAN. In order to perform the Mie scattering calculations several assumptions have been made beforehand. We assume that the aerosol particle size distribution can be described by a mono-modal log-normal distribution:

$$n(r) = \frac{N_0}{\sqrt{2\pi} \cdot \ln(S) \cdot r} \cdot \exp\left[-\frac{(\ln r - \ln r_m)^2}{2 \ln^2(S)}\right] \quad (1)$$

Here, N_0 is the total particle number density, r_m the median radius, r the particle radius and S represents the geometric standard deviation of the distribution, a measure of the distribution width (Grainger, 2017).

Mie simulations were carried out for various combinations of distribution width S , refractive index n_r and median radius r_m , as described in more detail below. The Mie scattering calculations were carried out using routines from the *Earth Observation Data Group (EODG)* of the *University of Oxford*, available as downloads (for the software *IDL*) on their website (<http://eodg.atm.ox.ac.uk/MIE/#intro>, last checked: September 4, 2020). The choice of input values for the refractive indices and the median radii were guided by previous studies and literature (e.g., Ehlers et al., 2014; Kravitz et al., 2012; Penndorf, 1953). In this study we examined real parts of the refractive index n_r between 1.3 and 1.5 and particle radii ranging from 25 to 3000 nm. The imaginary part of the refractive index was set to zero ($n_i = 0$).

Having calculated the extinction coefficients of the aerosol particles possibly leading to a blue Sun, the impact of these aerosols and of air molecules on the transmission of solar radiation through the atmosphere was determined using the radiative transfer model SCIATRAN (Rozanov et al., 2014). SCIATRAN was developed by the Institute of Environmental Physics (IUP) of the University of Bremen for the interpretation of remote sensing measurements in the UV-visible-NIR-SWIR spectral range. In the transmission modelling mode, SCIATRAN can be used to simulate the atmospheric transmission of sunlight reaching the Earth's surface. In addition to the light scattering and absorption due to atmospheric gases, an aerosol layer can be included in the calculations. This layer is represented by the calculated extinction coefficient spectra covering a certain altitude range. The viewing geometry is set up with SCIATRAN in a way that the imaginary observer on the Earth surface is looking directly into the Sun. The solar zenith angle (SZA) as well as the optical depth have to be considered as possible influencing factors. For more information on how to use SCIATRAN see the detailed *User's Guide* provided as a download on the website of IUP Bremen (IUP, 2018). The model output contains transmission values at different wavelengths and solar zenith angles. Using the *SORCE* solar irradiation spectrum (LASP, 2003) the resulting spectral distribution of solar radiation through an aerosol-loaded atmosphere can then be calculated.



2.2 Calculation and display of colour values

Whether the simulated spectral distribution of solar radiation transmitted to the Earth’s surface is perceived as blue by a human observer has to be simulated using a colour model. Most important to consider are the sensitivities of the cone cells located on the retina of the eye, which are responsible for colour perception. The sensitivities of the three types of cone cells are represented by colour matching functions developed by the *International Commission on Illumination (CIE)* in 1931, based on experiments of W. David Wright and John Guild from 1928 and 1931 (Simon, 2008). The colour matching functions $\bar{x}(\lambda)$, $\bar{y}(\lambda)$ and $\bar{z}(\lambda)$ are displayed in Fig. 1.

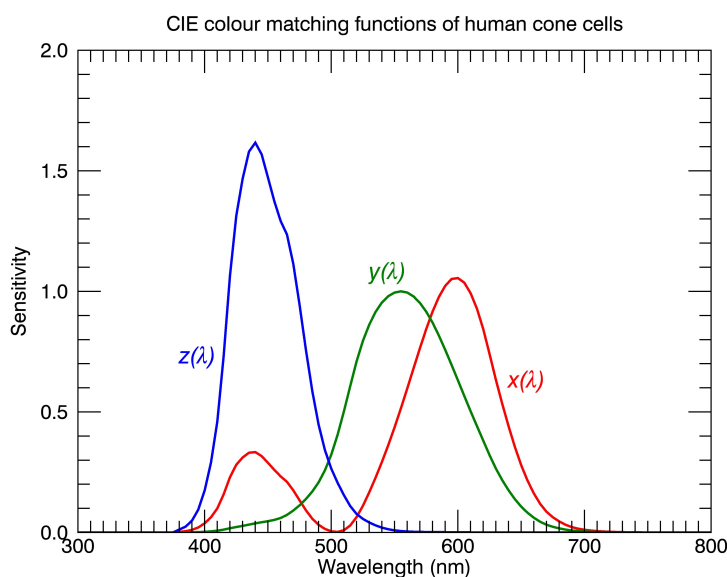


Figure 1. CIE colour matching functions of the human eye for the CIE 1931 2°- standard observer, after Judd (1951) and Vos (1978) (<http://cvrl.ioo.ucl.ac.uk/cmfs.htm>, last checked: September 4, 2020).

Combining these sensitivity curves with the incoming light’s spectral distribution $I(\lambda)$, the so-called XYZ tristimulus values can be calculated (see eqns. 2 – 4), as described by the CIE (2004).

$$100 \quad X = \int_{380nm}^{800nm} I(\lambda) \cdot \bar{x}(\lambda) \cdot d\lambda \quad (2)$$

$$Y = \int_{380nm}^{800nm} I(\lambda) \cdot \bar{y}(\lambda) \cdot d\lambda \quad (3)$$



$$Z = \int_{380nm}^{800nm} I(\lambda) \cdot \bar{z}(\lambda) \cdot d\lambda \quad (4)$$

In the current study we employ the CIE chromaticity values (x and y) determined from the XYZ tristimulus values to characterize the colour associated with a given transmission spectrum. The chromaticity values are determined in the following way:

$$x = \frac{X}{X + Y + Z} \quad (5)$$

$$y = \frac{Y}{X + Y + Z} \quad (6)$$

and are displayed in a 2-D x - y plot.

In addition we convert the tristimulus values to sRGB (standard RGB), which can be directly used to display colours in IDL (*Interactive Data Language*), the software used to prepare all Figures shown in this study. The conversion was done according to the *International Color Consortium (ICC)* (see Stokes et al., 1996) with a linear matrix transformation and a non-linear gamma correction. The colours of the monochromatic colour arc – shown in the panels of the right column of Fig. 3, which will be discussed in detail below – as well as the transmitted solar spectra were determined this way. The procedure was verified using several external routines. Different websites offer colour value calculators and the display of colours according to their sRGB-values (e.g., <http://www.brucelindbloom.com>, last checked: September 4, 2020); https://www.w3schools.com/colors/colors_rgb.asp, last checked: September 4, 2020).

3 Results

As mentioned above, in many previous studies on the origin of a blue moon or Sun, enhanced scattering of red light is provided as an explanation of the phenomenon. Usually, only scattering by the aerosol particles is considered, and Rayleigh scattering by air molecules is neglected. We start our considerations based on this assumption (Section 3.1) and then include a correct treatment of Rayleigh scattering based on SCIATRAN radiative transfer simulations in section 3.2.

3.1 Results without Rayleigh scattering and gaseous absorption

Previous studies, e.g., Penndorf (1953) suggest that the particle population leading to the blueing effect has a relatively narrow particle size distribution and a refractive index (real part n_r) of 1.3 to 1.5. Figure 2 shows the Mie extinction coefficient as a function of wavelength and median radius – normalized to the value at a reference wavelength of 350 nm – for two different distribution widths and for three different values of the real part of the refractive index. Results for a distribution width of S



= 1.05 (and $S = 1.2$) are shown in the top (bottom) row. The left, middle and right columns of the Fig. display results for refractive indices of (1.3, 0-i), (1.4, 0-i) and (1.5, 0-i), respectively.

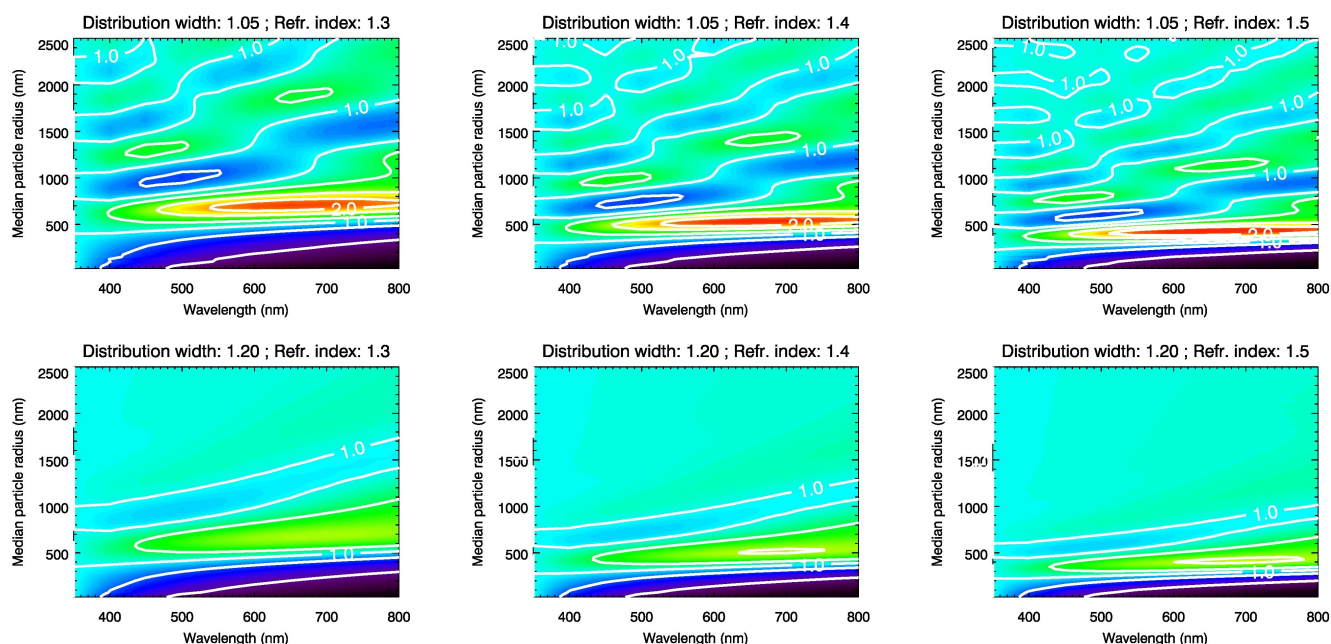


Figure 2. Spectral and radius dependence of aerosol extinction coefficients (normalized to 350 nm) determined by Mie-calculations assuming a mono-modal log-normal particle size distribution with a geometric width of $S = 1.05$ (top row) and $S = 1.2$ (bottom row) and real parts of the refractive index of 1.3 (left column), 1.4 (middle column) and 1.5 (right column). Contour levels are 0.3, 0.7, 1.0, 1.3, 1.7, 2.0, 2.3.

130 As can be seen in Fig. 2, maximum anomalous extinction is obtained under the assumptions made for median radii in the 400 – 700 nm range, with the specific values depending on the assumed refractive index. Two features of the plots are particularly noteworthy. First, the broader the size distribution, the less pronounced the anomalous extinction is (compare top and bottom row of Fig. 2). Secondly, the median radius producing the maximum anomalous extinction depends on the refractive index, decreasing from about 700 nm to about 450 nm as the real part of the refractive index increases from 1.3 to 1.5. In other words,
135 depending on the refractive index, particles of a slightly different size will more easily produce a blue Sun. It is also noticeable that a lower refractive index leads to a larger particle radius range with stronger anomalous scattering, making the blue Sun phenomenon more probable. Unfortunately, no aerosol samples have been taken and examined from past events, therefore the true value of the refractive index of the particles producing a blue Sun is unknown. Penndorf (1953) lists in his study on sightings of the blue Sun in 1950 products of biomass burning with a refractive index of around 1.46. In his calculations
140 however he uses the value of 1.33, based on the refractive indices of water and ice. Ball et al. (2015) have found real parts of refractive indices of volcanic ash of around 1.5. The results described in the following are based on a distribution width of $S = 1.05$ and a real part of the refractive index of 1.4, unless stated otherwise. These choices are arbitrary to a certain extent, but it



is impossible to present results for all possible parameter combinations. In addition, the main conclusions of the study are not affected by the specific values of the distribution width and refractive index chosen.

145 3.2 Rayleigh scattering and gaseous absorption

For the radiative transfer simulations carried out in this study, SCIATRAN version 3.8 (Rozanov et al., 2014) is used. Standard profiles of pressure, temperature and atmospheric trace gases for northern mid-latitudes taken from simulations with the Bremen 3-D CTM (Sinnhuber et al., 2003) are used, no clouds are included. Note that the choice of atmospheric background parameter profiles has a negligible effect on the results. SCIATRAN is run in *int - transmission - CDI* mode with refraction
150 switched on, simulating directly transmitted radiation to an observer on the Earth's surface (IUP, 2018; Rozanov et al., 2014). For the purpose of comparison with later findings, the results of the radiative transfer calculations and colour modelling of a Rayleigh-only atmosphere – i.e., without aerosols – are shown in Figure 3. This Figure is discussed now in more detail, because the following Figures are structured in the same way. The different rows of Fig. 3 show results for different SZAs (30° , 60° , 80° and 90°). The left column displays solar transmission spectra determined by multiplying the SORCE solar irradiance
155 spectrum (LASP, 2003) by the transmission spectrum simulated with SCIATRAN. The plots in the right column of Fig. 3 show the chromaticity values x and y determined as described above. This is a standard way to depict colour information. The arc with the filled colour circles represents the positions of the corresponding monochromatic spectra in the x - y -plane. The colours of the circles are based on the conversion of the chromaticity values to sRGB as described in section 2.2. The smaller open circle annotated by “ S_0 ” corresponds to the chromaticity values of the unattenuated solar spectrum. The larger circle displays
160 the position and the colour of the corresponding transmission spectrum in the x - y -plane. The colour of the Sun changes from whitish-yellowish for small SZAs to orange for $SZA = 90^\circ$, as expected. This is easily explained by the λ^{-4} dependence of Rayleigh scattering (Strutt, 1871), i.e., radiation with shorter wavelength (blue light) is scattered more strongly than radiation with longer wavelengths. The pathlength of light through the atmosphere increases with increasing SZA, and the impact of Rayleigh scattering also increases, leading to an orange sunset which can be seen in the lowest panel of Fig. 3 where the Sun
165 is at the horizon.

3.3 Simulation of a blue Sun

For the Sun to appear blue, the spectral irradiance values and therefore the transmission must be higher at shorter wavelengths relative to longer wavelengths in the visible spectral range. To reach this, in the following an aerosol layer was inserted into the model atmosphere and the radiative transfer calculations were repeated. Previous studies as well as the contour plot in Fig. 2
170 suggest that particles with a median radius of 400 – 700 nm (depending on the refractive index) are able to cause a blue Sun. In this study different particle sizes in the range from 25 to 3000 nm have been tested and Rayleigh scattering taken into account. Fig. 4 shows results in a similar way as Fig. 3, but with an aerosol layer in 6 – 8 km altitude, an optical depth of $\tau = 1$, a real part of the refractive index of 1.4, median radius $r_m = 550$ nm and a distribution width of $S = 1.05$. Note that the layer altitude was found to have only a minor effect on the results, except for large solar zenith angles (see also section 4). According to Fig.
175 2 this set of parameters is associated with close to the maximum possible anomalous extinction in the visible spectral range.

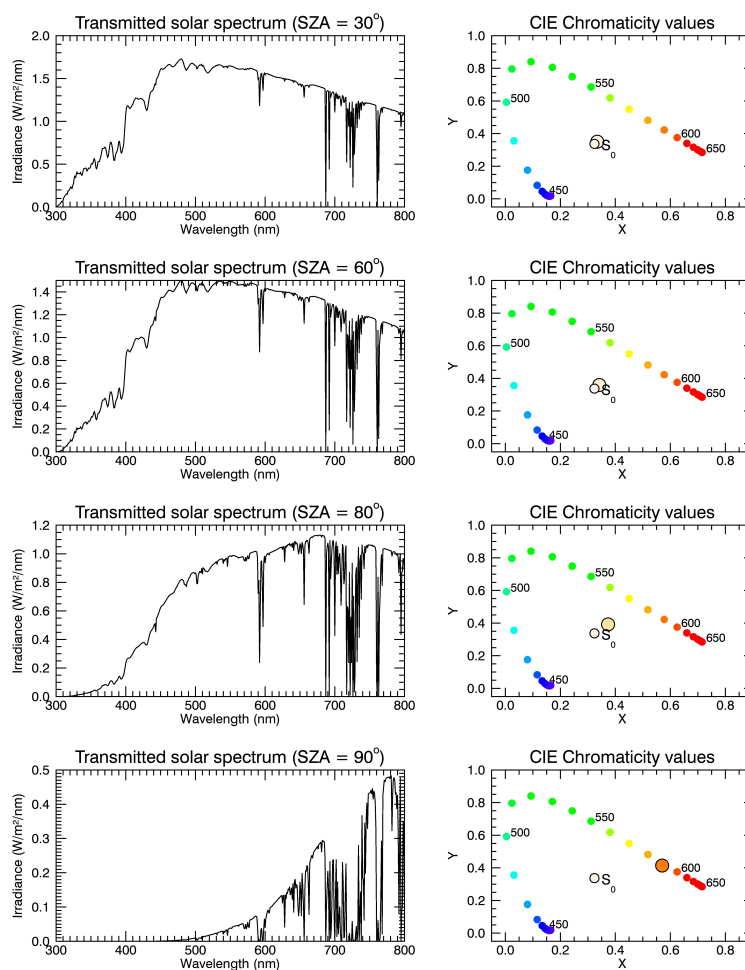


Figure 3. Results for an atmosphere without aerosols. The plots in the left column show the solar transmission spectra simulated for solar zenith angles of 30°, 60°, 80° and 90°, respectively (top to bottom), while the diagrams in the right column show the corresponding CIE chromaticity plots. The transmission spectra are calculated for an observer at the Earth’s surface (0 m a.s.l.) looking directly into the Sun.

Fig. 4 shows that these assumptions lead to a blue colour of the Sun. Even for the smallest SZA of 30° a light blue colouring of the Sun occurs. For the largest SZAs shown, the Sun assumes a deep blue colour. For increasing optical depth, the blueing effect is more pronounced for all SZAs, the transmission is further reduced and for an optical depth of, e.g., $\tau = 2$ the Sun assumes an indigo colour for SZAs of 80° and 90° (not shown). Another aspect that must be considered is that colours may not be perceived if the transmitted solar radiation is too weak. According to Horvath et al. (1994), colour perception will not work if transmission values are smaller than about 10^{-7} , which puts additional constraints on the combination of parameters producing a blue sun.

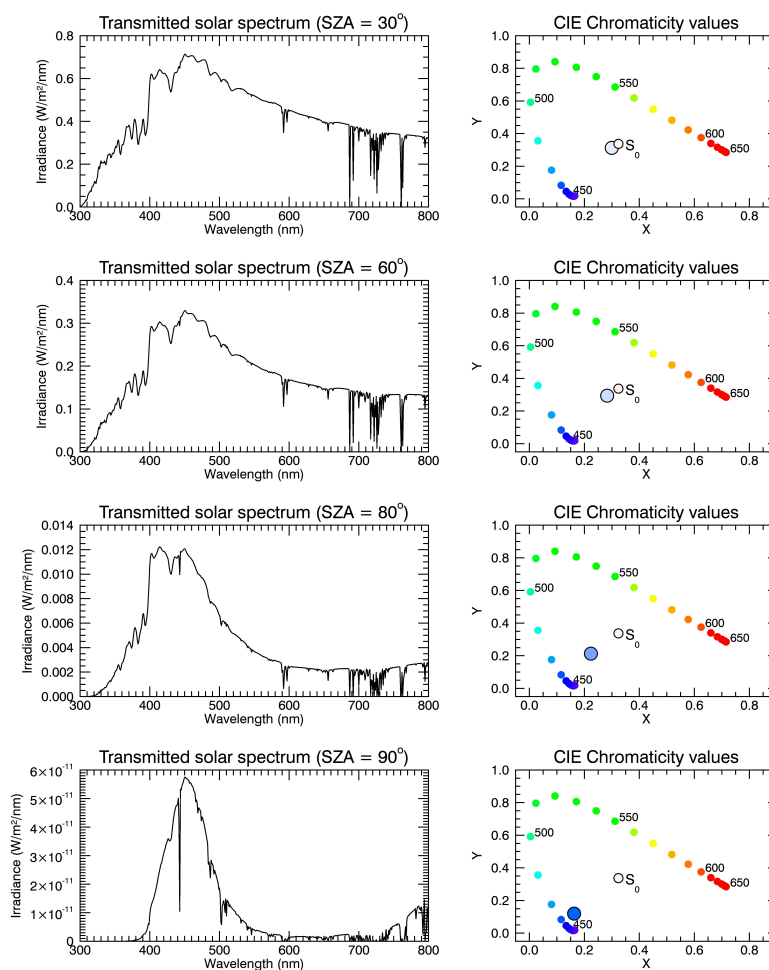


Figure 4. Simulated transmission spectra (left column) and CIE chromaticity plots (right column) for a ground-based observer looking directly into the Sun and for SZAs of 30°, 60°, 80° and 90° (from top to bottom). The simulations include Rayleigh scattering, molecular absorption by all relevant species and an additional aerosol layer with anomalous extinction and a vertical optical depth of $\tau = 1$ (at 550 nm), a distribution width of $S = 1.05$, a real part of the refractive index of 1.4 and a median radius of $r_m = 550$ nm. A blue Sun can be reproduced with the assumptions made for all SZAs considered.

3.4 Impact of particle size

Based on the results shown in Fig. 2, significant anomalous extinction in the optical spectral range can only be produced for a relatively narrow particle size distribution and for specific particle sizes, represented here by the median radius of a mono-modal log-normal distribution. Figure 5 shows chromaticity diagrams for different SZA and median radius values, for an aerosol layer with an optical density of $\tau = 1$, a height of 6 – 8 km and a refractive index of $n = 1.4 + i \cdot 0$. For a median radius of r_m of 350 nm (first column of Fig. 5) the aerosol extinction coefficient decreases with increasing wavelength for the



refractive index assumed here (see also Fig. 2) and the aerosol layer amplifies the effect of Rayleigh scattering and leads to
190 a red Sun. Note that our results nicely confirm the general notion that Rayleigh scattering only will only produce an orange
sun during sunset (see Fig. 3), while aerosols with of a sufficiently small size are required for red sunsets (left column of Fig.
5). The results for $r_m = 150$ nm (not shown) are quite similar to the results for $r_m = 350$ nm. The second column shows the
results for $r_m = 550$ nm, i.e., the median radius roughly associated with the most extreme anomalous extinction for a refractive
index (real part) of 1.4, according to Fig. 2. A blue Sun can clearly be modelled with this set of parameters. Interesting are the
195 results for a median radius of 750 nm (third column), which show a more and more green Sun with increasing SZA. For $r_m =$
950 nm (last column) the modelled Sun becomes again orange-red for the largest SZA, consistent with the spectral dependence
displayed in Fig. 2.

3.5 Aerosol scattering vs. Rayleigh scattering

As in most earlier studies on the phenomenon of the blue Sun Rayleigh scattering was not properly taken into account, it
200 is worthwhile to investigate, how the results change, if Rayleigh scattering is switched off in the RT model. The results for
an aerosol layer in 6 – 8 km altitude with an optical depth of $\tau = 1$, median radius $r_m = 550$ nm, distribution width $S =$
1.05 and without Rayleigh scattering are shown in Fig. 6. Apparently and as expected, a blue Sun is more easily produced
without Rayleigh scattering for all SZAs. Ignoring Rayleigh scattering, a blue Sun can be simulated for optical depths as low
as approximately $\tau = 0.1$ for $r_m = 550$ nm, $S = 1.05$ and $n_r = 1.4$ (results not shown). If Rayleigh scattering is considered,
205 an aerosol optical depth of at least $\tau = 0.5$ is required to cause a blueing of the Sun. Note that depending on the specific set
of aerosol parameters chosen, there are very large differences in CIE chromaticity values and colour, depending on whether
Rayleigh scattering is considered or not. Unfortunately, only a fraction of the simulations carried out can be shown here.

One possibility to reduce the impact of Rayleigh scattering in the real atmosphere is to observe from higher altitudes, e.g.,
from an aircraft (e.g., Horvath et al., 1994). Under these conditions – and an aerosol layer occurring above the observer –
210 Rayleigh scattering is significantly reduced, providing more favorable conditions for a blue Sun to occur.

3.6 Case study: Results by Wilson (1951)

Among the available studies on the 1950 Canadian forest fires (e.g., Schüepp, 1950; Ångström, 1951; Ditzel, 1951; Gelbke,
1951; Jenne, 1951; Wilson, 1951; Penndorf, 1953), the work by Wilson (1951) is particularly noteworthy and relevant, because
it contains a measured spectrum of transmitted visible radiation for a blue Sun scenario, obtained on September 27, 1950 from
215 Edinburgh. The author also took measurements of a “normal” Sun spectrum at the same solar zenith angle, which allows the
determination of the slant aerosol optical depth. Interestingly, the blue Sun and the normal Sun spectrum shown in Wilson
(1951) (see Plate 8 on page 478) exhibit unexpected spectral features – maxima near 450 nm and 550 nm and a pronounced
minimum around 490 nm – that differ significantly from the transmission spectra simulated in the present study (see also Fig.
8). We currently do not have a convincing explanation for these spectral features. The slant aerosol optical depth spectrum for a
220 SZA of 71° based on the analysis of Wilson (1951) is shown in Fig. 7. It should be mentioned that Fig. 7 shows the optical depth
in the sense of Beer-Lambert’s law, i.e., $\tau = -\ln \frac{I}{I_0}$ and not the quantity shown in Fig. 1 of Wilson (1951). Note that spectral

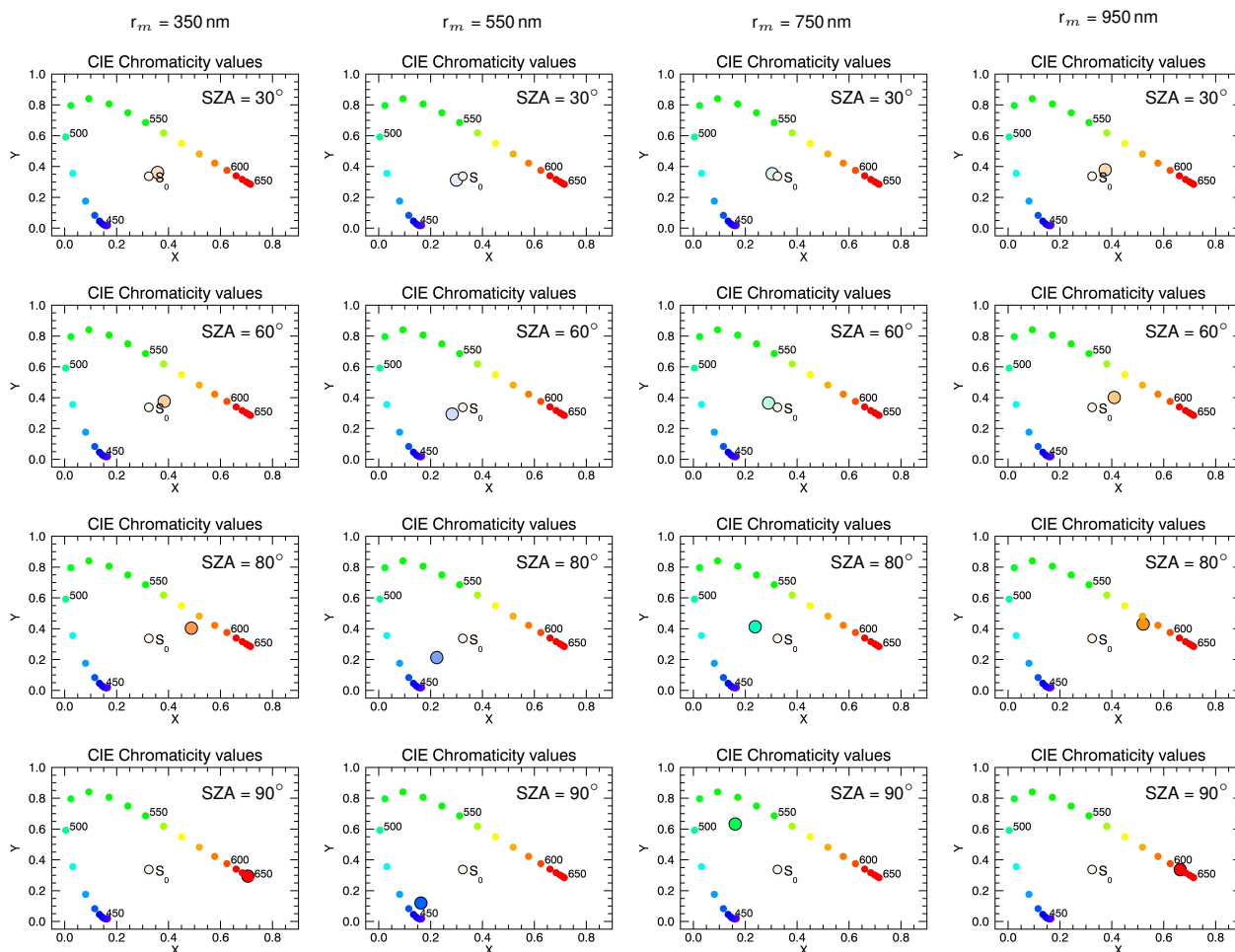


Figure 5. Chromaticity diagrams for different combinations of SZA and median radius r_m of the mono-modal log-normal particle size distribution. Results for SZAs of 30° , 60° , 80° and 90° are shown in the different rows of the Figure, whereas the columns show results for r_m of 350 nm, 550 nm, 750 nm and 950 nm. All results are for a distribution width of $S = 1.05$, a real part of the refractive index of 1.4, aerosol optical depth of $\tau = 1$ and an aerosol layer in the 6 – 8 km altitude range.

measurements are only available in the spectral range from 381 nm to 633 nm. Apparently, the optical depth increases from 450 to 650 nm, but the relative variation is with about 10% not very large. Using the optical depth spectrum we performed radiative transfer simulations for the solar zenith angle ($SZA = 71^\circ$) of the blue Sun measurement by Wilson (1951) with SCIATRAN in order to test, whether this optical depth spectrum does indeed produce a blue Sun. The aerosol layer was assumed to occur in 10 – 12 km altitude, following Penndorf (1953). The vertical aerosol optical depth in this case was $\tau \approx 3.2$ at 550 nm based on the slant optical depth reported by Wilson (1951) and converted to vertical optical depth using SCIATRAN. The results are shown in Fig. 8 including Rayleigh scattering (top row) and without Rayleigh scattering (bottom row). A light blue colour of the Sun is already visible in the top row, i.e., including Rayleigh scattering, but the effect is more pronounced without Rayleigh

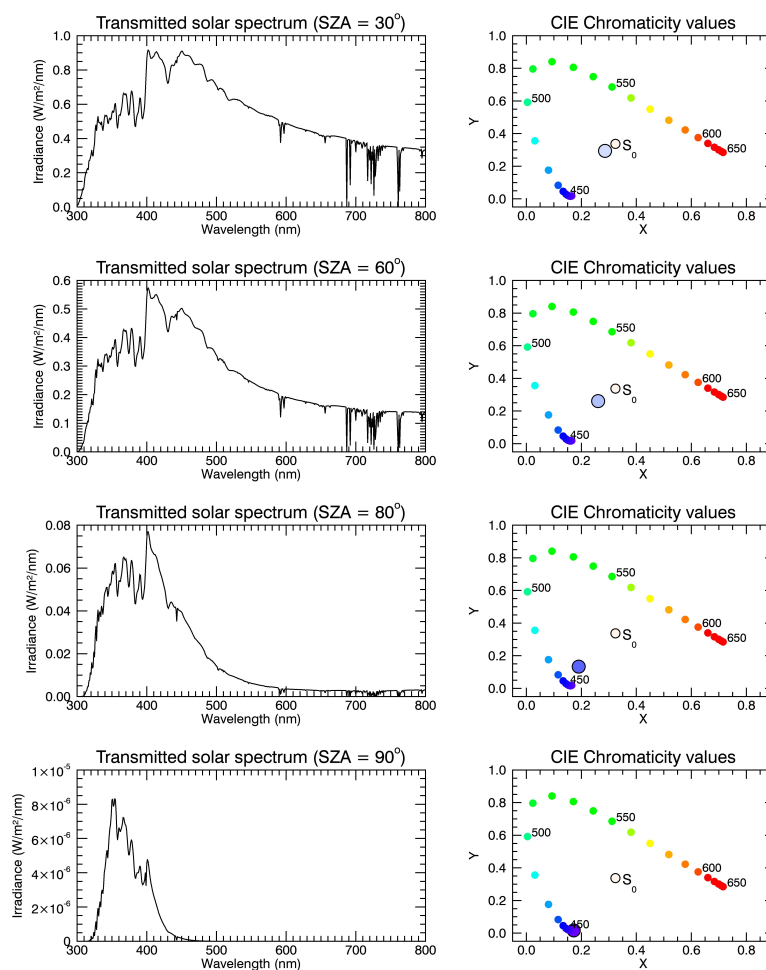


Figure 6. Similar to Fig. 4, but with Rayleigh scattering switched off. All other parameters are identical as in Fig. 4, i.e., $\tau = 1$, $r_m = 550$ nm, $S = 1.05$, layer altitude 6 – 8 km.

230 scattering – as expected – again demonstrating that correct treatment of Rayleigh scattering is important. Neglecting Rayleigh
scattering shifts the spectral maximum to slightly shorter wavelengths. With a slant optical depth of 9 – 10 (as in Fig. 7), solar
radiation is attenuated by 4 – 5 orders of magnitude.

It is also noteworthy that Gelbke (1951) presented a photograph of the blue sun – taken from Greifswald, Germany by W.
Gelbke on September 27, 1950, i.e., one day after the spectral measurement by Wilson (1951) – which, to our knowledge, is
235 the only available photograph of the event.

The simulations show that the aerosol optical depth spectrum determined by Wilson (1951) does indeed allow simulating
a blue Sun, despite the questionable spectral signatures in the solar transmission spectra. A plausible explanation for these
spectral signatures may be that both the “blue Sun” and the “normal Sun” spectra presented by Wilson (1951) were affected by

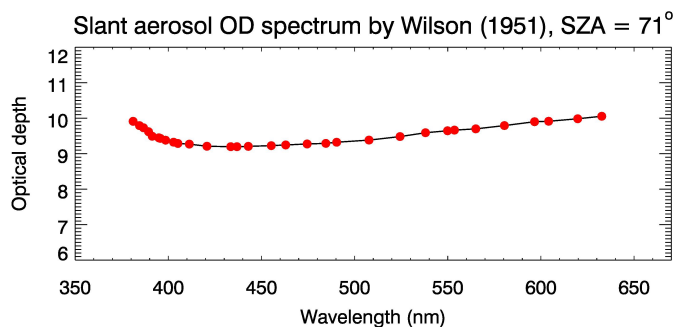


Figure 7. Spectrum of slant aerosol optical depth based on the analysis by Wilson (1951).

the same or very similar systematic effects that largely cancelled out when taking the ratio of the two spectra. The results also demonstrate that a blue Sun can be reproduced even with a small relative spectral variation of the aerosol optical depth in the visible spectral range.

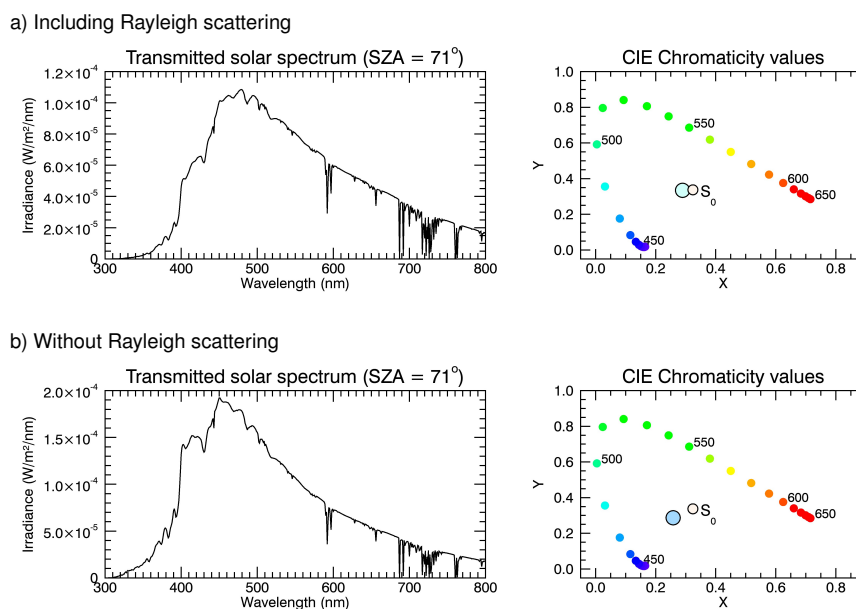


Figure 8. Similar to Figure 4, but for the aerosol optical depth and aerosol extinction spectrum taken from Wilson (1951) including Rayleigh scattering (top row) and without Rayleigh scattering (bottom row).



3.7 The role of absorption by H₂O

Several observers took measurements of the spectral distribution of transmitted solar radiation during the green or blue Sun events in the aftermath of the 1883 eruption of Krakatoa (Symons et al., 1888). The red part of the spectrum was found to be markedly suppressed. The Fraunhofer A line (at 760 nm, caused by O₂) could not be observed during the events and the Fraunhofer B line (at 687 nm, also caused by O₂) was difficult to observe and was not discernible for SZAs approaching 90° (Symons et al., 1888, p. 212). The observers reported unusually strong absorption by “water” (or water vapour), and absorption by water vapour was also discussed as a potential explanation of the blue Suns after the Krakatoa eruption (Symons et al., 1888).

The effect of H₂O vapor absorption on the transmission spectra and the resulting colour of the Sun was also tested using SCIATRAN. For tropospheric H₂O mixing ratios of 4% – which is often considered the upper limit in the troposphere – and an aerosol-free atmosphere, a blue colour of the Sun can not be reproduced (results not shown, but they are close to the results for the aerosol-free case shown in Fig. 3). Even for a tropospheric H₂O mixing ratio of 40% – which is utterly unrealistic – the Sun appears yellowish and turns orange for large SZAs. We therefore exclude absorption by H₂O as a sole explanation for blue Suns. However, absorption of solar radiation by H₂O may contribute to the blue colour, if scattering aerosols are present in the atmosphere. One may expect that high H₂O mixing ratios lead to smaller aerosol optical depths required to produce a blue colour of the Sun, because H₂O absorbs strongly in the red part of the visible spectrum.

4 Discussion

In this study we investigated the influence of aerosol particles with different size distributions and refractive indices on the colour of the Sun, as perceived by a ground-based human observer. Different factors were examined that may be able to evoke a shift in the transmitted solar spectral distribution towards a higher intensity at shorter wavelengths in the blue region of the visible spectrum.

It is obvious that a suppression of red light – relative to the shorter wavelengths – is the key prerequisite for producing a blue Sun or a blue moon. In principle this may be caused by molecular extinction or extinction by aerosol particles. Molecular extinction can be excluded as a cause (see also section 3.7). Extinction by aerosol particles may in principle be caused by scattering or absorption of radiation by the aerosol particles. In all previous attempts to explain the phenomenon of the blue Sun, absorption by aerosols has been dismissed and we believe this was done for good reasons. Absorption coefficients of essentially all different types of aerosols, including mineral dust and volcanic ash decrease with increasing wavelength in the visible spectral range. Bergstrom et al. (2007) report on measurements of spectral absorption properties of the most important absorbing aerosol types, including biomass burning aerosols, desert dust, pollution and mixtures, which consistently yield positive Ångström exponents, i.e., extinction coefficients (or optical depth) decreasing with increasing wavelength. Patterson (1981) reported on measurements of the imaginary part of the refractive index of volcanic ash emitted during the Mount St. Helens eruption in 1980. The imaginary part decreases with increasing wavelength in the 300 nm – 700 nm spectral range, and so does the absorption cross section (or coefficient). Patterson et al. (1983) reported similar measurements of the ash emitted



275 by the El Chichon eruption in 1982 and found similar results. Pollack et al. (1973) reported measurements of the imaginary part of the refractive index of five different rock types. In some cases the imaginary part n_i of the refractive index was found to be increasing with increasing wavelength in the visible spectral range. However, it has to be kept in mind that the absorption coefficient is proportional to the ratio of n_i and the wavelength $k_{ext} \propto \frac{n_i}{\lambda}$. This again leads to k_{ext} decreasing with increasing wavelength. To summarize, absorption by aerosol particles appears to be an unlikely cause of the blue Sun phenomenon.

280 The results presented so far were mostly for an aerosol layer in 6 – 8 km altitude, which is certainly arbitrary. Simulations were also carried out for aerosol layers in 2 – 4 km and 10 – 12 km altitude. We generally found little dependence of the results on layer altitude, except for SZAs approaching 90° . At these large SZAs the blueing effect on the Sun gets more pronounced the lower the aerosol layer is (results not shown). It is beyond the scope of this study to present all cases in detail.

It should be pointed out that our results confirm the basic notion of previous studies, that anomalous scattering in the visible
285 spectral range caused by a suitably sized aerosol population is able to explain the occurrence of a blue or green Sun. A narrow aerosol particle size distribution with an appropriate mean or median radius will more easily lead to blue Suns compared to a broader size distribution. One general question is, how a narrow size distribution can be achieved in the real atmosphere. One possibility could be a size separation by sedimentation, perhaps accompanied by different wind directions at different altitudes, as already suggested by Gelbke (1951). The right combination of conditions for the occurrence of a blue Sun can be expected
290 to arise only rarely, which provides an explanation for the infrequent observations of a blue Sun.

5 Conclusions

We investigated possible reasons for the occurrence of a blue Sun, including anomalous scattering by suitably sized aerosols, aerosol absorption and absorption by water vapour. This study included – for the first time to our best knowledge – a comprehensive treatment of Rayleigh scattering in simulations of a blue Sun. Depending on the specific aerosol and observational
295 parameters (SZA), Rayleigh scattering was found to have a significant impact on the simulated colour of the Sun. Anomalous extinction is more pronounced for narrow aerosol particle size distributions (given the right aerosol size), but the investigations based on the aerosol optical depth retrieved by Wilson (1951) demonstrated that a relatively weak increase in aerosol extinction with wavelength in the visible spectral range also allows simulating a blue Sun. This implies that blue Suns can also be produced for somewhat broader size distributions. Our results indicate that an aerosol optical depth of about 0.5 is sufficient
300 to explain a blue Sun, if the aerosol size parameters are chosen in an optimal way. If Rayleigh scattering is neglected – which is unrealistic, but has been done in many earlier studies – an aerosol optical depth of only 0.1 is sufficient to yield a blue Sun. Absorption by water vapour – also proposed as a potential explanation for the blue Sun phenomenon – was shown to be a very unlikely explanation. This study confirms the result of several other studies, that anomalous extinction by aerosol particles of a specific size and size distribution allows explaining the occurrence of blue or green Suns. However, Rayleigh scattering should
305 not be neglected.



Author contributions. CvS outlined the project, NW carried out the initial SCIATRAN simulations with guidance by AR and implemented the colour display approach. NW also wrote an initial version of the manuscript. AL and CvS improved the analyses and extended the manuscript. All authors discussed, edited and proofread the paper.

Competing interests. The authors declare that they have no competing interests.

310 *Code availability.* The SCIATRAN radiative transfer model can be downloaded from the following website: <https://www.iup.uni-bremen.de/sciatran/>.

Acknowledgements. This work was supported by the Deutsche Forschungsgemeinschaft (project VolARC of the DFG research unit VolImpact FOR 2820, grant no. 398006378). We are indebted to the Institute of Environmental Physics of the University of Bremen – particularly to Dr. Vladimir Rozanov and Prof. Dr. John P. Burrows FRS – for access to the SCIATRAN radiative transfer model.



315 References

- Ångström, A.: The Blue Sun of September 1950, *Tellus*, 3(3), 135 – 140, doi:10.3402/tellusa.v3i3.8635, 1951.
- Ball, J. G. C., Reed, B. E., Grainger, R. G., Peters, D. M., Mather, T. A., and Pyle, D. M.: Measurements of the complex refractive index of volcanic ash at 450, 546.7, and 650 nm, *J. Geophys. Res. Atmos.*, 120, 7747 – 7757, doi:10.1002/2015JD023521, 2015.
- Bauch, M.: The Day the Sun Turned Blue: A Volcanic Eruption in the Early 1460s and Its Possible Climatic Impact – A Natural Disaster Perceived Globally in the Late Middle Ages?, in: Schenk, Gerrit J. (ed.), *Historical Disaster Experiences. A Comparative and Transcultural Survey between Asia and Europe*, Heidelberg, 107 – 138, 2017.
- Bergstrom, R. W., Pilewskie, P., Russell, P. B., Redemann, J., Bond, T. C., Quinn, P. K., and Sierau, B.: Spectral absorption properties of atmospheric aerosols, *Atmos. Chem. Phys.*, 7, 5937 – 5943, doi:10.5194/acp-7-5937-2007, 2007.
- Commission Internationale De L'Eclairage (CIE): CIE 15: 2004 – Colorimetry 3rd edition, Technical Report, 2004.
- 325 Ditze, G.: Die anormale Trübung der Atmosphäre September/Oktober 1950, *Zeitschrift f. Meteorologie*, 5(3), 86 – 87, 1951.
- Ehlers, K., Chakrabarty, R., and Moosmüller, H.: Blue moons and Martian sunsets, *Appl. Opt.*, 53(9), 2014.
- Gelbke, W.: Bemerkungen zum Phänomen der blauen Sonne, *Zeitschrift für Meteorologie*, 5(3), 82 – 84, 1951.
- Grainger, R. G.: *Some Useful Formulae for Aerosol Size Distributions and Optical Properties*, Earth Observation Data Group, University of Oxford, 2017.
- 330 Horvath, H., Metzig, G., Preining, O., and Pueschel, R. F.: Observation of a blue sun over New Mexico, U.S.A., on 19 April 1991, *Atmos. Env.*, 28(4), 621 – 630, 1994.
- Institute of Environmental Physics/Institute of Remote Sensing (IUP/IFE), University of Bremen, Germany: User's Guide for the Software Package SCIATRAN (Radiative Transfer Model and Retrieval Algorithm) – Version 3.8, <http://www.iup.uni-bremen.de/sciattran/> (last checked: September 4, 2020), 2018.
- 335 Jenne, W.: Das Phänomen "Blaue Sonne", *Tellus*, 3(3), 129 – 134, doi:10.3402/tellusa.v3i3.8636, 1951.
- Judd, D. B.: Report of U.S. Secretariat Committee on Colorimetry and Artificial Daylight, In *Proceedings of the Twelfth Session of the CIE*, Stockholm (Vol. 1, pp. 11), Paris: Bureau Central de la CIE, 1951.
- Kiessling, J.: *Untersuchungen über Dämmerungserscheinungen*, Voss, Hamburg und Leipzig, 1888.
- Kravitz, B., MacMartin, D. G., and Caldeira, K.: Geoengineering: Whiter skies?, *Geophys. Res. Lett.*, 39, L11801, doi:10.1029/2012GL051652, 2012.
- 340 Larrabee, W. H.: Green suns and red sunsets, *Popular Science Monthly*, 24, 1884.
- Laboratory for Atmospheric and Space Physics (LASP): SORCE Solar Spectral Irradiance, Spectrum. LASP Interactive Solar Irradiance Data Center (LISIRD), University of Colorado, http://lasp.colorado.edu/lisird/data/sorce_ssi_13/, (last checked: September 4, 2020), 2003.
- Mie, G.: Beiträge zur Optik trüber Medien, speziell kolloidaler Metallösungen, *Annalen der Physik*, 25:377, 1908.
- 345 Patterson, E. M.: Measurements of the Imaginary Part of the Refractive Index Between 300 and 700 nm for Mount St. Helens Ash, *Science*, 211, 836 – 838, 1981.
- Patterson, E. M., Pollard, C. O., and Galindo, I.: Optical properties of the ash from El Chichon volcano, *Geophys. Res. Lett.*, 10(4), 317 – 320, 1983.
- Penndorf, R.: On the phenomenon of the colored sun, especially the blue sun of september 1950, Technical Report 20, Air Force Cambridge Research Center (U.S.), Geophysics Research Directorate, 1953.
- 350 Pollack, J. B., Toon, O. B., and Khare, B. N.: Optical Properties of Some Terrestrial Rocks and Glasses, *Icarus*, 19, 372 – 389, 1973.



- Porch, William M., Ensor, David S., Charlson, Robert J., and Heintzenberg, Jost: Blue Moon: Is it a Property of Background Aerosol?, *Appl. Opt.*, 12(1), 1973.
- 355 Rozanov, V., Rozanov, A., Kokhanovsky, A., and Burrows, J.: Radiative transfer through terrestrial atmosphere and ocean: Software package SCIATRAN, *J. Quant. Spec. Rad. Trans.*, 133, 13 – 71, 2014.
- Schüepp, W.: Beitrag zum Phänomen der blauen Sonne, *Experientia*, 6, 457 – 459, doi:10.1007/BF0215410, 1950.
- Sinnhuber, B.-M., Weber, M., Amankwah, A., and Burrows, J. P.: Total ozone during the unusual Antarctic winter of 2002, *Geophys. Res. Lett.*, 30, 1580, doi:10.1029/2002GL016798, 2003.
- 360 Simon, K.: *Farbe im Digitalen Publizieren - Konzepte der digitalen Farbwiedergabe für Office, Design und Software*, Springer-Verlag Berlin Heidelberg, 2008.
- Stokes, M., Anderson, M., Chandrasekar, S., and Motta, R.: *A Standard Default Color Space for the Internet: sRGB*, International Color Consortium (ICC), 1996.
- Strutt, J. W. (1871), On the light from the sky, its polarization and colour, *The London, Edinburgh, and Dublin Philosophical Magazine and Journal of Science*, 41(271), 107 – 120, doi:10.1080/14786447108640452, 1871.
- 365 Symons, G., Judd, J., Strachey, R., Wharton, W., Evans, F., Russell, F., Archibald, D., and Whipple, G.: *The Eruption of Krakatoa: And Subsequent Phenomena*, Krakatoa Committee of the Royal Society (Great Britain), 1888.
- Vos, J. J.: Colorimetric and photometric properties of a 2-deg fundamental observer, *Color Research and Application*, 3, 125 – 128, 1978.
- Wilson, R.: The blue sun of 1950 september, *Monthly Notices of the Royal Astronomical Society*, 111(5), pp. 478–489, 1951.